



Published in final edited form as:

J Immunol. 2012 September 15; 189(6): 3178–3187. doi:10.4049/jimmunol.1201053.

Microbial Carriage State of Peripheral Blood Dendritic cells (DCs) in Chronic Periodontitis Influences DC Differentiation, Atherogenic Potential[†]

Julio Carrion, DDS, PhD¹, Elizabeth Scisci, BS¹, Brodie Miles, BS², Gregory J. Sabino, PhD¹, Amir E Zeituni, PhD¹, Ying Gu, DDS, PhD¹, Adam Bear, DDS¹, Caroline A Genco, PhD³, David L. Brown, MD⁴, and Christopher W Cutler, DDS, PhD^{1,5,‡}

¹Stony Brook University School of Dental Medicine, Stony Brook University, NY

²Department of Molecular Genetics and Microbiology, Center for Infectious Diseases, Stony Brook University, Stony Brook, NY

³Department of Medicine, Section of Infectious Diseases and Department of Microbiology, Boston University School of Medicine

⁴Department of Cardiology, School of Medicine, Stony Brook University, Stony Brook

⁵Georgia Health Sciences University- College of Dental Medicine

Abstract

The low grade oral infection chronic periodontitis (CP) has been implicated in coronary artery disease risk, but the mechanisms are unclear. Here, a pathophysiological role for blood dendritic cells (DCs) in systemic dissemination of oral mucosal pathogens to atherosclerotic plaques was investigated in humans. The frequency and microbiome of CD19–BDCA-1+DC-SIGN+ blood myeloid DCs (mDCs) were analyzed in CP subjects with, or without existing acute coronary syndrome (ACS) and in healthy controls (CTL). FACS analysis revealed a significant increase in blood mDCs in the following order: CTL<CP<ACS/CP. Analysis of the blood mDC microbiome by 16s rDNA sequencing showed *Porphyromonas gingivalis* and other species, including (cultivable) *Burkholderia cepacia*. The mDC carriage rate with *P. gingivalis* correlated with oral carriage rate and with serologic exposure to *P. gingivalis* in CP subjects. Intervention (local debridement) to elicit a bacteremia increased the mDC carriage rate and frequency *in vivo*. *In vitro* studies established that *P. gingivalis* enhanced by 28% the differentiation of monocytes into immature mDCs; moreover, mDCs secreted high levels of MMP-9 and upregulated C1q, HSP60, HSP-70, CCR2 and CXCL16 transcripts in response to *P. gingivalis* in a fimbriae-dependent manner. Moreover, the survival of the anaerobe *P. gingivalis* under aerobic conditions was enhanced when within mDCs. Immunofluorescence analysis of oral mucosa and atherosclerotic plaques demonstrate infiltration with mDCs, colocalized with *P. gingivalis*. Our results suggest a role for blood mDCs in harboring and disseminating pathogens from oral mucosa to atherosclerosis plaques, which may provide key signals for mDC differentiation and atherogenic conversion.

[†]This study was supported by US Public Health Service grants from the NIH/NIDCR (K23 DE018187 to J.C., R01 DE014328, R21 DE020916 to C.W.C., F31 DE020014 to A.E.Z, F30 DE021649-01 to E.S.)

[‡]Address correspondence and reprint requests to: Dr. Christopher W. Cutler, Department of Periodontics, College of Dental Medicine, Georgia Health Sciences University; 1120 15th Street, Augusta, GA. 30912-1220., Phone# 706-721-2442, Fax# 706-723-0215, chcutler@georgiahealth.edu.

Disclosures

The authors have no financial conflicts of interest

Keywords

blood dendritic cells; *Porphyromonas gingivalis*; atherosclerosis; chronic periodontitis; acute coronary syndrome

Introduction

Coronary artery disease (CAD) and its thrombotic complications are currently the most deadly and disabling cardiovascular diseases in affluent countries. CAD is the leading cause of mortality in the United States, and it is believed that CAD will continue to spread globally unless improved methods are developed to identify at-risk individuals (reviewed in (1) and institute preventive measures.

The most commonly recognized risk factors for CAD include diabetes, smoking, hypertension and hyperlipidemia (2). Chronic low grade infections with bacterial species *Chlamydia pneumoniae*, *Helicobacter pylori*, *Porphyromonas gingivalis* and others are also suspected of conferring increased CAD risk (3, 4); however, the mechanisms are not clear.

Chronic periodontitis (CP) is a low grade infection identified as a risk factor for CAD (5, 6) (4) and other systemic diseases (7). The oral submucosa in CP is a niche for growth of oral gram-negative anaerobes such as *P. gingivalis*. *P. gingivalis* is uniquely able to infect myeloid DCs and reprogram them to induce an immunosuppressive T effector response (8–10). *P. gingivalis* has been identified in bacteremias (11) (12) and atherosclerotic plaques in humans (13) moreover, it accelerates atherosclerosis in ApoE $-/-$ mice in a manner that is dependent on expression of fimbrial adhesins (4).

Invasion of the arterial vessel walls by inflammatory cells is indispensable to CAD development. Infiltrating cells include monocytes/macrophages (14, 15) lymphocytes, neutrophils and myeloid DCs (mDCs) (16, 17). An emerging body of literature supports a pivotal role for mDCs in CAD development in humans (18) and mice (19, 20), as reviewed in (21). However, the predominant sources of mDCs in atherosclerotic plaques and the factors that trigger their activation, infiltration and differentiation remain elusive.

Circulating DCs called ‘blood DCs’ and their progenitors are likely sources of infiltrating DCs in CAD (22). In humans, blood DC subsets include CD123+ CD303+ plasmacytoid DCs, CD19 $-$ CD1c+ (BDCA-1) mDCs and a minor subset of CD141+ mDCs (23). Blood DCs are derived from bone marrow progenitors, monocytes and ostensibly, DC-SIGN+ tissue DCs that have reverse transmigrated into circulation after capture of microbial antigens (24, 25). Previous work has documented mDCs actively infiltrating the oral submucosa in CP (26) (27) and rupture-prone atherosclerotic plaques (28). However, the role of blood mDCs in clearance of bacteremias and dissemination to distant sites such as atherosclerotic plaques is undocumented in humans.

In the present study we show that blood mDCs of humans with CP harbor microbes identified in oral mucosa and atherosclerotic plaques. MDCs provide these microbes with a protective niche and mode of transport. The microbe in turn stimulates differentiation of mDCs from monocytes and converts mDCs into an atherogenic phenotype.

Methods and Materials

Study Population

The Committee on Research Involving Human Subjects (CORIHS) at Stony Brook University approved all protocols involving human subjects. Informed consent was obtained

from all subjects before commencement of the study. The cohort of subjects with chronic periodontitis (CP) consisted of 40 subjects with moderate to severe CP as determined by the presence of greater than 20 teeth, of which at least 8 exhibited: probing depth > 4mm, attachment loss > 3mm, bleeding on probing, alveolar bone crest > 3 mm from cemento–enamel junction (CEJ). Demographic data and clinical parameters of the study subjects are shown in Table 1. Exclusion criteria included: steroidal anti-inflammatory agents, smoking, periodontal treatment within the past 6 months, pregnancy, diabetes, heart disease, or cancer. After the initial exam, all CP patients were subjected to scaling and root planing (local debridement of the root surfaces and pockets) under local anesthesia and the blood mDC response evaluated at 24 hours. A subset of CP subjects included those with acute coronary syndrome (ACS) (n=15), diagnosed as reported (29) and shown in Table 1. ACS subjects without CP could not be identified. Healthy controls (CTL) consisted of 25 age and gender-matched subjects, non-smokers without CP; who had no history of ACS, diabetes, cancer or other reported systemic disease. Healthy controls were not subjected to scaling and root planing because there is no clinical need and it can be detrimental to clinical attachment levels.

Blood mDC isolation

Peripheral blood mononuclear cells (PBMCs) were isolated from 30ml of whole blood and a nucleated cell suspension was prepared using Ficoll-Paque Plus density gradient centrifugation (GE Healthcare). Myeloid DCs (mDCs) were isolated by positive immunoselection as described previously (30). Briefly, PBMCs labeled with BDCA-1 (CD1c)-PE⁺ (BDCA-1., Miltenyi Biotec Cat. no. 130-090-508), CD209-APC⁺ (BD Cat. No. 551545), CD19-FITC⁺ (BD Cat. No. 557697) were FACsorted (FACS ARIA-BD Biosciences) then sorted again to remove CD19⁺ (B⁻) cells. These procedures routinely yielded mDC (CD1c⁺CD209⁺CD19⁻) preparations of >95% purity.

Generation of monocyte derived dendritic cells (MoDCs)

To serve as *in vitro* model of DC infectivity and *P. gingivalis* survival, MoDCs were generated as we have described previously (9, 27, 31). Briefly, monocytes were isolated from mononuclear cell fractions of the peripheral blood of healthy controls and seeded in the presence of GM-CSF (100 ng/ml, PeproTech Inc. Cat # 300-03) and IL-4 (25 ng/ml, R&D Systems Cat# 204-IL-010) at a concentration of $1-2 \times 10^5$ cells/ml for 6–8 days, after which flow cytometry was performed to confirm the immature DC phenotype (CD14⁻CD83⁻CD1a⁺CD1c⁺DC-SIGN⁺ (all antibodies from BD Biosciences, except CD1c [Miltenyi Biotec])).

In vitro infection and mDC differentiation model

After PBMC isolation and plastic adherence, monocytes were scraped off plates and collected. The total number of monocytes was counted using Accuri's C6 Flow Cytometer® System and baseline levels of CD14, CD1c, DC-SIGN, CD86 and CD83 expression were obtained. Monocytes were then divided equally into 6-well plates and treated either with GM-CSF and IL-4 alone, wild-type Pg381 alone, GM-CSF and IL-4 plus wild-type Pg381, or RPMI alone. Bacterial multiplicities of infection (MOIs) chosen were 0.1, 0.5, and 1. Each experimental condition was performed in triplicate. Cells for each condition were collected on subsequent days 1, 2, and 3 for analysis of MoDCs present and changes in receptor expression. Cells were gated on scattergram plots based on size characteristics for both monocytes and MoDCs. Flow samples were collected based on total number of events rather than volume, so differentiation of monocytes into dendritic cells is represented as MoDCs per microliter of sample. Triplicates were averaged and assembled onto a line graph to show the differentiation of monocytes to MoDCs with and without growth factors. Intensity profiles of CD14, DC-SIGN, CD1c, and CD83 expression were compared with

baseline monocyte levels to show downregulation of CD14, upregulation of DC-SIGN and CD1c and immature state of MoDCs (CD83–CCR7–) for each condition.

Flow cytometric phenotyping

MDCs were labeled with combinations of PE-, FITC-, allophycocyanin (APC) and PerCP mouse anti-human lineage Ab (CD14, CD19, CD11b/Mac-1, CD1c [BDCA-1, Miltenyi Biotec], CD80, CD83, CD86, HLA-DR, CD209 (DC-SIGN), CD1a or isotype controls (all from BD-Biosciences, San Jose, CA); and Goat Anti-Mouse IgG (H+L) [Invitrogen]. Analysis was performed with a FACSCalibur flow cytometer (BD). Marker expression was analyzed as the percentage of positive cells in the relevant population defined by forward scatter and side scatter characteristics. Expression levels were evaluated by assessing mean fluorescence intensity indices calculated by relating the mean fluorescence intensity noted with the relevant mAb to that of the isotype control mAb for samples labeled in parallel and acquired using the same setting.

Blood mDC frequency change after treatment

Blood PBMCs were obtained from all study subjects at baseline and 24 hours after a single intensive bout of scaling and root planing (S&RP), as reported (32). This treatment has previously been shown to result in acute, short term bacteremia (33, 34), as well as systemic inflammation (32) The mDCs were labeled with fluorescent conjugated antibodies (as described above), CD19–CD1c+DC-SIGN+ sorted (FACS Aria-BD) and analyzed (FACS Diva v.6.1.3) as described above.

Quantitative RT-PCR and DNA Sequencing

Quantitative RT-PCR—To detect and quantitate *P. gingivalis*, genomic DNA (gDNA) and total RNA was isolated from subgingival plaque and mDCs with the RNeasy Micro kit (QIAGEN) according to the manufacturers' instructions, but with a slight modification. Briefly, gDNA Eliminator spin columns were not used during the isolation protocol. This was done to collect, in addition to total RNA, gDNA for *P. gingivalis* 16S rDNA detection in the mDCs. cDNA was synthesized using STR1 Enhanced Avian First Strand Synthesis Kit (Sigma-Aldrich Cat. No. STR1-1KT). The cDNA template was standardized to a concentration of 0.1 µg/µl using a NanoDrop 3300 Fluorospectrometer (Thermo-Scientific Cat. No. ND3300) with Quant-iT™ dsDNA HS Assay Kit (Invitrogen Cat. No. Q32851). Quantitative real time-PCR (qRT-PCR) was used to detect the presence of *P. gingivalis* (16S rDNA) in MoDCs, mDCs and dental plaque samples. The 16S rDNA consisted of a forward *Pg*-specific primer (5'-TGT AGA TGA CTG ATG GTG AAA ACC-3' and a universal reverse primer (C11R), 5'-ACG TCA TCC CCA CCT TCC TC-3' sequence as previously described (35). The universal reverse primer was also used to detect non-*P. gingivalis* amplification products, which were then subjected to genomic blast sequencing. PCR reactions were performed using QuantiTect SYBR Green PCR Kit (Qiagen Cat. No 204145) on a iCycler Thermal Cycler (Biorad). The thermal cycling conditions were an initial incubation step of 15 minutes at 95°C to activate HotStartTaq DNA polymerase. This step prevents the formation of misprimed products and primer-dimers during reaction setup and the first denaturation step, leading to high PCR specificity and accurate quantification. This initial incubation step was followed by 45–50 cycles at 94°C for 15 s, 54 °C for 30 s and 72 °C for 30 s. *P. gingivalis* 16s rDNA primer was a kind gift of Dr. Stephen Walker, SUNY-Stony Brook, NY. As a quantitative standard for qRT-PCR analysis of mDCs, MoDCs were spiked *in vitro* with *P. gingivalis* 381 at a range of multiplicity of infections (MOI) and colony forming units per ml (CFU/ml). This yielded a linear regression curve consisting of log₁₀ CFU/ml vs. amplification cycles (Supplementary Figure 1C). The infection status of mDC from the blood was then expressed as estimated CFU/ml and MOI relative to our

MoDC standard. In order to confirm the specificity of the PCR amplified product using the *P. gingivalis* 16S rDNA primer, (or the non-*P. gingivalis* specific PCR amplified products) the resultant amplicons were sequenced. Briefly, the amplified product was run in a 1% agarose gel electrophoresis (Bio-Rad Cat. No. 162-0102) along with an 0.1–10.0kb DNA ladder (New England BioLabs Cat. No N3200S). The resultant band was extracted and purified from the agarose gel using QIAEX II Gel Extraction Kit (Qiagen Cat. No. 20051), according to the manufacturer's instructions. The DNA template (3.0 ng) were combined with 3.2 pmol 16S rDNA primer and sequenced using a 3730 DNA Analyzer (Applied Biosystems). The sequenced product was then aligned against all human, prokaryotic and eukaryotic known database genome using Genomic BlastSequence (BLASTN 2.2.24+) (http://www.ncbi.nlm.nih.gov/sutils/genom_table.cgi).

Intracellular Survival

Wild type Pg381 was used to infect MoDCs, or PMNs at a multiplicity of infection of 100. Uptake of the bacteria by human cells was confirmed by observing complete internalization of CFSE-stained *P. gingivalis* via epifluorescence microscopy as soon as 60 minutes after inoculation. Cells were then washed twice in PBS and re-suspended in culture medium for continued incubation. At each time point, cells were re-suspended in sterile water on ice for 20 minutes to initiate cell lysis. Remaining bacteria released from within the cells was re-suspended in PBS, and streaked on anaerobic 5% blood agar plates in triplicate under anaerobic conditions (10% H₂, 5% CO₂ in nitrogen) at a one in ten dilution. Plates were incubated in anaerobic conditions at 35 C for 14 days after which colonies were numerated and surviving cell forming units per mL were determined.

Derivation of monoclonal antibody to DC invasin, mfa-1 minor fimbriae

MAb 89.15 against the DC-invasin, mfa-1 (minor fimbriae) was generated by the Cell Culture/Hybridoma Facility at Stony Brook University. Briefly, three female 6–8 week old BALB/c mice (Charles River) were immunized intraperitoneally with three 50 µg doses of native minor fimbriae (Mfa-1) in Sigma adjuvant (Sigma-Aldrich Co., St. Louis, MO) at two-week intervals, following which sera was drawn and tested by enzyme-linked immunosorbent assay (ELISA) for the presence of antigen-specific antibodies. The mouse selected for splenectomy had a titer of >1:1000 to the protein. Prior to fusion, the mouse was boosted intraperitoneally with 1 µg of Mfa-1 in PBS (Gibco-Invitrogen, Carlsbad, CA). Four days following the booster, the mouse was sacrificed, the spleen cells isolated aseptically and fused with mouse myeloma cell line Sp2/0 (ATCC), as described (36). Clones were screened by ELISA against native minor fimbriae. Clones were then further screened using a whole bacteria ELISA against MFI, which expresses only the major fimbriae (Pg min⁻/maj⁺), and DPG3, which expresses only the minor fimbriae (Pg min⁺/maj⁻). Clone 89 was determined to be positive both by native minor fimbria ELISA and whole bacteria ELISA and thus was selected for sub cloning by limiting dilution. Sub clone 89.15 was selected by ELISA for further study. MAb 89.15 was determined to be of the IgG1 isotype having a κ light chain, by use of the IsoStrip Mouse Monoclonal Antibody Isotyping Kit (Roche Applied Science, Indianapolis, IN). Antibodies from this sub clone are referred to as AEZαMfa1.

Immunofluorescence staining of oral mucosal tissues and coronary artery tissues

Oral mucosal tissues from the human gingiva were collected from untreated CP patients using a biopsy technique previously reported (37). Immediately after collection, the tissues were rinsed with sterile saline to remove traces of blood and embedded in Tissue Tek OCT compound (Sakura) and snap frozen in liquid nitrogen, and sectioned into 7 µM thick sections using a cryostat (Leica CM1850). Coronary artery tissues were obtained from human post-mortem patients with atherosclerosis (ATH) and CP (kind gift from Dr. Emil

Kozarov, Columbia University, NY) and cryosectioned as described above. For immunofluorescent staining, sections were fixed in acetone for 5 min at -20°C , rehydrated in PBS lacking Ca^{+2} and Mg^{+2} (PBS-), blocked with 5% bovine serum albumin (BSA; Sigma-Aldrich) in PBS- along with anti-human FcR block reagent (Miltenyi Biotec, Auburn, CA) for 1 h, and washed. Sections were incubated for 30 min at RT with conjugated primary antibodies diluted in PBS-, and washed before mounting. All sections were mounted with VectaShield mounting medium containing 4',6-diamidino-2-phenylindole (DAPI) (Vector Laboratories, Inc., Burlingame, CA). To identify DC-SIGN within arterial plaques and gingival tissue sections, fluorescein isothiocyanate (FITC)-conjugated (BioLegend, San Diego, CA.) or RPE-conjugated mouse anti-human CD209 (AbD Serotec, Raleigh, NC) were used. FITC-conjugated mouse anti-human CD1c was used (BD Biosciences) to identify CD1c. DyLight™ microscale antibody labeling kit (Thermo Scientific, Rockford, IL) was used to conjugate Alexa Fluor 594 to mfa-1 antibody AEZαMfa1 according to manufacturer's protocol. Controls included isotype matched antibodies and pre-immune antibodies. Images were acquired with a Zeiss LSM 510 META NLO Two-Photon Laser Scanning Confocal Microscope System coupled with image processor software for image processing. In addition, sections were stained with hematoxylin and eosin stain (H&E) to examine cell and tissue morphology. The H & E images were analyzed by image enhanced light microscopy (Nikon E600).

In situ association of mDCs with *P. gingivalis* by immunofluorescence

mDCs from blood of CP and ACS/CP patients were analyzed by immunofluorescence cytometry to determine infection with *P. gingivalis*. Briefly, FACS-sorted CD19–CD1c+Dc-SIGN+ mDCs were permeabilized and fixed in Shandon Cytospin Collection Fluid (Thermo Scientific Cat. No. 6768315). The cytological specimen was deposited on Ultrastick slides (Thermo Scientific Cat. 3039) and cytocentrifuged (Shandon Cytospin 4, Thermo Scientific, Inc). After blocking human FcR, as described above, mDCs were probed with PE-AEZαMfa1 and Vectashield™ mounting media with DAPI (VWR Cat. No. 101098-044) was added to the specimens and then slides were analyzed by conventional epifluorescence (Nikon E600) and by confocal microscopy as above.

Quantitation of serum DC-poietins FLT3-ligand, sTNF RI, sTNF RII

Serum analysis of DC-poietin levels was conducted with colorimetric sandwich ELISA using respective Quantikine Immunoassays: Human Flt-3 Ligand (Quantikine DFK00), sTNF RI (Quantikine DRT100), sTNF RII (Quantikine DRT200) (R&D Systems). Briefly, standard dilutions and recommended serum sample dilutions were incubated in pre-coated microplates containing a specific monoclonal antibody. Unbound debris was washed and an enzyme-linked polyclonal antibody specific for the target molecule was added. Unbound antibody was removed and a substrate solution was added to give a proportionate color change relative to the amount of DC-poietin in the well. The substrate reaction was stopped and microplates were read immediately at 450nm on a microplate reader with a correction wavelength of 540nm (EMax, Molecular Devices).

Determination of human anti-*Porphyromonas gingivalis* IgG titers

Serum levels of anti-*P. gingivalis* IgG antibodies were determined by ELISA as previously described (38). In brief, 96-well ELISA plates were coated with *P. gingivalis* strain DPG-3 (1×10^7 cells/well), followed by one hour incubation at 37°C . The wells were blocked for 2 hours at 37°C with 2% bovine serum albumin (Sigma Chemical Co., St. Louis, MO, USA; Cat. No. A3912) in PBS-tween20 (Sigma Chemical Co., St. Louis, MO, USA; Cat. No. P1379). Appropriate dilution of serum samples as determined by checkerboard titrations using pooled sera was added and the plates were incubated for 2 h at 37°C . Horseradish peroxidase (HRP)-conjugated goat anti-human IgG (H+L) antibodies (Promega, Madison,

WI, USA; Cat. No. W4031) were added and incubated for 1 h at 37°C. TMB (3,3',5,5'-Tetramethyl-benzidine Liquid Substrate for ELISA, Sigma Chemical Co., St. Louis, MO, USA; Cat. No. T4444) was used as a substrate. The reaction was stopped by the addition of 3N hydrochloric acid (LabChem Inc., Pittsburgh, PA, USA; Cat. No. LC15360-2), and the optical density were read using an E-max microplate reader (Molecular Devices, Palo Alto, CA, USA) at 450 nm.

Statistical analysis

Summary statistics were computed for human peripheral blood myeloid DC counts (numbers and percentages), number of PBMCs, serum IgG titers, serum DC poietins and lipid profiles in humans, who were grouped according to disease status. D'Agostino-Pearson normality test at $p < 0.05$ was performed to confirm Gaussian distribution, after which differences in means \pm S.D. of healthy vs. CP or ACS/CP and CP vs. ACS/CP subjects were analyzed by Students t-test at $p < 0.05$ (GraphPad Prism 5, GraphPad Software, Inc, La Jolla, CA 92037 USA). The incidence of *P. gingivalis* in subgingival plaque and blood mDCs of CP patients was analyzed by Chi-square and Fishers's exact test, and Spearman rank test (shown) with significance assessed at $p < 0.05$. In vitro assays of DC differentiation, DC expression of MMP-9 and fold-changes in atherogenic marker mRNA were performed in triplicate and repeated a minimum of three times. Data were analyzed either by repeated measures ANOVA or Kruskal-Wallis test at $p < 0.05$.

Results

Blood mDC frequency increases with chronic periodontitis (CP), acute coronary syndrome (ACS)

The number and percentages (Figure 1) of blood mDCs were analyzed in three groups: healthy controls (CTL), CP subjects at increased coronary artery disease risk due to lipid profile and serologic exposure to the atherogenic pathogen *P. gingivalis* (Table 1) (39) and 100% coronary artery disease risk due to existing ACS, as well as CP. No ACS patients could be found without CP. The results show significant increases in blood mDCs in the following order: CTL < CP < ACS/CP. This was not attributable to an increase in total peripheral blood mononuclear cells (PBMCs), which were actually decreased in CP and ACS/CP (Figure 1B.3). Due to previous correlation between blood DC frequency and serum levels of FLT-3L and soluble TNF receptors (40) (41), we analyzed these cytokines in the same patient sera. The results show no difference in FLT-3L, TNFr1 or TNFr2 in CP vs. CTL subjects. However, a significant increase was noted in all three cytokines in ACS/CP, relative to CP and CTL ($p < 0.05$, Students t-test) (Figure 1C). As infectious seropositivity has been correlated with cardiovascular disease mortality (42) we analyzed the correlation between serum antibody titers against *P. gingivalis* DPG-3, a strain that solely expresses the DC adhesin, mfa-1 fimbriae (9) and blood mDC numbers. The results demonstrate a linear relationship between serum antibody titers to *P. gingivalis* DPG-3 and blood mDC frequency in CTL vs CP ($r^2 = 0.56$, $p < 0.0001$). (Supplementary Figure 1A). Note that sera and subgingival plaque from the ACS/CP cohort were unavailable for analysis here, but previous studies have documented in ACS subjects, the presence of serum IgG antibodies to *P. gingivalis* and *P. gingivalis* DNA in saliva (43)

Blood mDCs contain a microbiome, as well as viable pathogens and intact *P. gingivalis*

To determine if the blood mDCs contain microbes that could help explain their responsiveness *in vivo*, blood mDCs were isolated from CP and ACS/CP subjects and analyzed by 16s rDNA- sequencing, immunofluorescence and viable cultures. The 197 bp amplified product specific for *P. gingivalis* is shown in representative mDCs of CP and ACS/CP subjects, relative to *in vitro* controls (Supplementary Figure 1B). Overall, 72% of

CP subjects who were orally colonized by *P. gingivalis* (Supplementary Table 1) were also positive for *P. gingivalis* 16s rDNA within blood mDCs, while no CTL mDCs yielded the amplified product. The correlation between oral colonization with *P. gingivalis* and mDC infection rate in CP subjects was positive and significant (Spearman $r = 0.5192$, $p = 0.0078$). Although dental plaque was unavailable from ACS/CP patients for analysis, 37.5% of their mDCs were positive for *P. gingivalis* 16s rDNA. To estimate the level of *P. gingivalis* infection of blood mDCs, MoDCs were pulsed with a range of known MOIs and CFUs of *P. gingivalis* and 16s rDNA used to generate linear regression models (Supplementary Figure 1C, Supplementary Table 1). Based on these models, we calculated estimated CFUs (eCFU) of *P. gingivalis* in blood mDCs from CP and ACS/CP patients, which were equal to 132,623 eCFUs ($\pm 121,484$ S.E.), while estimated MOIs were all below 1. Other species identified and sequenced from 16s rDNA of mDCs included *Helicobacter pylori*, *Pseudomonas spp.*, *Moraxella catarrhalis*, *Klebsiella pneumonia* and *Salmonella enterica* and others. Live bacteria recovered on blood agar from mDCs included *Burkholderia cepacia* from two ACS/CP patients (Supplementary Table 1). Although viable *P. gingivalis* were not cultivable from blood mDCs, probably due to their dormant state (44) we did identify intact *P. gingivalis* at low MOI within mDCs of CP subject by immunofluorescence-confocal microscopy (Figure 2A). The specificity of our monoclonal antibody for *P. gingivalis* mfa-1 (AEZ α Mfa1) was first established as shown (Supplementary Figure 1D). To confirm the ability of *P. gingivalis* to infect CD1c⁺ DC-SIGN⁺ blood mDCs, we pulsed *ex vivo* isolated mDCs from a CTL subject with CFSE-labeled *P. gingivalis in vitro*, which were then counterlabeled with DC-SIGN. The results show intact *P. gingivalis*-CFSE within DC-SIGN⁺ blood mDCs (Figure 2B).

Induction of short-term bacteremia increases blood mDC carriage state and frequency

To determine if elevated peripheral blood DC counts correlated with the presence of blood-borne infection, CP patients were subjected to mechanical debridement (i.e. scaling and root planing or S&RP), the standard therapy for CP. This treatment is well documented to drive oral bacteria such as *P. gingivalis* and others into the bloodstream (32) (11) (33). MDCs were isolated 24 hours later and analyzed for *P. gingivalis* 16s rDNA content and blood mDC frequency. The results (Figure 2C) indicate a significant increase in *P. gingivalis* content of blood mDCs after S&RP. Accompanying this was a ~25% increase in blood mDC frequency (Figure 2D). This response was statistically significant when comparing pre- and post-treatment in all the CP subjects ($p < 0.05$, paired students t-test) (Figure 2E). There was no increase in total PBMCs after therapy, nor were levels of DC-poetins FLT-3L, TNFr1 or TNFr2 significantly altered by therapy (data not shown).

Increased mDC frequency involves de novo mDC differentiation in response to infection

A previous *in vitro* study indicated that differentiation of DCs from monocytes can be enhanced by antibody ligation of DC-SIGN (45). We reasoned that a similar ligation of DC-SIGN by *P. gingivalis* mfa-1, as reported (10) may enhance differentiation from monocytes. Therefore, monocytes were cultured with the growth factors GM-CSF/IL-4 and *P. gingivalis* added at low MOIs in select wells. The results confirmed that GM-CSF/IL-4 alone promotes differentiation of monocytes into immature CD1c⁺ DC-SIGN⁺ mDCs, after an apparent one day delay. These were indeed immature mDCs, as they were negative for CD83 and CCR7 (not shown). Moreover, mDC differentiation was enhanced $\approx 28\%$ by *P. gingivalis* at an MOI of 0.1, but was retarded by MOI of 0.5 and 1 in a dose dependent manner (Figure 3A). Interestingly, *P. gingivalis* alone at 0.1 MOI induced differentiation of CD1c⁺ DC-SIGN⁺ mDCs in the absence of GM-CSF/IL-4 (Figure 3B), and this continued for three days. When the MOI dose was increased to 0.5, the effect was diminished, while at an MOI of 1 caused no enhancement of MoDC differentiation relative to controls.

MDCs provide a protective niche for *P. gingivalis*

Viable *P. gingivalis* (44) and *Chlamydia pneumonia* (46) have been recovered with some difficulty from atherosclerotic plaques. To determine whether the obligate anaerobe *P. gingivalis* survives within mDCs under aerobic conditions, *in vitro* culture studies were performed. Our results (Figure 3C) show that *P. gingivalis* survives for 24 hrs within mDCs, while it dies rapidly in the absence of mDCs. Pre-treatment of mDCs with cytochalasin D reduces the protective effect of mDCs ten-fold at 6 hrs and 24 hrs. We further show professional phagocytes PMNS kill *P. gingivalis* rapidly.

Conversion of mDCs to atherogenic phenotype by DC invasive *P. gingivalis*

Matrix metalloproteinases (MMPs) are involved in extracellular matrix destruction, in plaque rupture and myocardial infarction (47). MMP-9 is particularly important in mDC migration (48). We therefore analyzed secretion of MMP-9 by mDCs pulsed with *P. gingivalis* strains that express the DC adhesin mfa-1 and gain access into mDCs (i.e. Pg381, PgDPG-3) or not (PgMFI). The results support mfa-1-dependent secretion of MMP-9 by mDCs (Figure 3D). Other indicators of risk of plaque rupture, including C1q (49), HSP60/HSP70 (reviewed in (50), CCR2 (51) and CXCL16 (52) (53) were analyzed at the mRNA level (Figure 3E). Analysis of these transcripts indicates that C1q, HSP60, HSP-70, CCR2 and CXCL16 are upregulated in response to fimbriated Pg381, relative to untreated control. Moreover, relative to the fimbriae-less mutant Pg MFB, Pg381 upregulates C1q, CXCL16 and HSP-70 on mDCs.

MDCs infected by *P. gingivalis* infiltrate oral submucosa and atherosclerotic plaques in situ

Previous quantitative immunofluorescence histomorphometry established that the diseased oral mucosa (26, 54) and atherosclerotic plaques (16) are infiltrated with increasing numbers of DC-SIGN+ mDCs. In view of the current data and our previous *in vitro* work establishing mfa-1 fimbriae as a DC-SIGN (CD209) ligand (9, 10) we opted to ascertain whether mfa-1 could be identified within DC-SIGN+ and CD1c+ mDCs in oral mucosa. The results indicate that *P. gingivalis* mfa-1 colocalizes with DC-SIGN+ mDCs in oral submucosa (Figure 4). Identical staining of healthy control (oral) tissue revealed trace mfa-1 and some DC-SIGN positivity, but no mfa-1/DC-SIGN colocalization was detected (not shown). We then probed post-mortem coronary artery biopsies from patients with CAD and CP using the same antibodies (Figure 5). A representative sample is shown. Note erosion and vascular inflammation of the intimal subendothelial layer (box) (Figure 5A). Evident are CD1c+ (Figure 5B) and DC-SIGN+ (Figure 5C) mDCs, as well as colocalization of *P. gingivalis* mfa-1 with its receptor DC-SIGN (Figure 5D).

Discussion

Here we provide evidence in humans for infection of mDCs as a significant route for pathogen dissemination to atherosclerotic plaques. The blood DCs respond to the low-grade infection CP, as well as the acute bacteremia elicited by treatment of CP. DCs were first identified in the human aortic intima in 1995 and were thought to be important in the development of atherosclerotic lesions (18). Soon after, DCs were shown to contact T cells and to overexpress, in early lesions, heat shock protein-70 (HSP-70), an indicator of physiologic stress (55). Hsp-70 is also expressed by intracellular bacterial species (56) including *P. gingivalis* (57) and as we show here, by mDCs infected with *P. gingivalis*. Subsequent studies of atherosclerotic plaques showed a prodigious infiltrate of DC-SIGN+ immature mDCs (58), as we observed in oral mucosa of CP subjects (54). The immature state of these mDCs is consistent with a reported role for DC-SIGN ligation in inhibiting TLR-mediated DC maturation (9, 59) and in promoting differentiation of immature DCs

from progenitors (45). The present work isolated CD1c⁺DC-SIGN⁺ mDCs from the blood of patients at increased risk for CAD and those with existing CAD and showed that they harbor DNA of *P. gingivalis* and other human pathogens. The infection of blood mDCs was linked to increased blood mDC frequency and to increased relative risk of CAD. The blood mDCs were immature despite containing whole intact *P. gingivalis*. This is consistent with inefficient maturation of mDCs by *P. gingivalis* due to ligation of DC-SIGN by mfa-1 (9). The initial site of mDC infection by *P. gingivalis* is most likely the oral submucosa. Introduction of *P. gingivalis* into the oral mucosa in mice results in rapid (30 min) bacteremia (personal communication from C.A. Genco), but the role of DCs in this bacteremia is not yet clear. Trafficking of mDCs through tissues is aided, in particular, by matrix-metalloproteinase 9 (MMP-9) (48, 60), a biomarker of increased CAD risk and a mediator of plaque instability (61). We show that human mDCs stimulated by *P. gingivalis* release high levels of MMP-9, and that this is dependent on expression by *P. gingivalis* of the DC-invasin mfa-1. Increased mobilization of Langerhans cells, which express CD1c (55) and dermal DCs, which express DC-SIGN, is observed in the oral submucosa in CP and these DCs accumulate in close proximity to the vasculature (27, 54). Hypoxic conditions, as in the subgingival pockets where *P. gingivalis* resides (62) promote the transmigratory activity of DCs through endothelium (63). Overall, the hypoxic microenvironment and local infection with *P. gingivalis* may be a potent driving force for reverse transmigration of tissue mDCs into the blood to atherosclerotic plaques (8, 25, 64).

Our findings also shed light on the enigmatic functions of blood DCs. It has been speculated that blood DCs translocate antigenic material from its point of origin to remote target tissues (25). Our results suggest that clearance of bacteremias may be a pathophysiological function of blood DCs. Bacteremia is a well-described phenomenon in patients with CP (33), and is induced by eating an apple (12), tooth brushing, flossing, or undergoing S&RP (65). We demonstrate that both the chronic condition CP and acute bacteremia increases the *P. gingivalis* content of blood mDCs and results in an increase in blood mDC frequency. Other infectious conditions that alter DC frequency include tuberculosis (66), malaria (67) and filariasis (68). We initially suspected that DC poietin levels were altering blood mDC frequency in CP, as reported in a number of diseases including CAD in humans (40, 66)(69), (41),(70), (71), (72), (73), (74). While elevated DC poietins were found in sera of our ACS/CP cohort, all had been on long-term cardiovascular care, including lipid lowering drugs. These are known to raise mDC levels (73). Moreover, 100% of our ACS cohort had CP; none could be identified without it. It should be noted that our systemically healthy CP cohort were not on such drugs and DC poietin levels were unchanged in CP. We therefore surmised that the bacteremia itself was the impetus for increasing mDC frequency. We thus implemented an *in vitro* infection assay to ascertain the mechanism. We show that indeed DC differentiation was enhanced by *P. gingivalis* at low MOIs, but retarded at higher MOIs. We surmise that this differential response may be reflective of a balance between two driving forces. At low MOIs, the DC-SIGN ligand *P. gingivalis* mfa-1 (10) positively influences DC differentiation, as reported for anti-DC-SIGN antibodies (45). This involves activation of a unique signaling pathway, the DC-SIGN signalosome, which is counterregulatory to TLR signaling (59). In contrast, infection by *P. gingivalis* at higher MOIs has a negative influence on DC differentiation due to enhanced apoptosis (75). While we have no evidence yet that this effect is specific for *P. gingivalis*, previous studies using several other species suggest a predominantly negative influence of bacterial infection on DC differentiation (76).

Collectively, these data indicate that mDCs in tissues and blood harbor pathogens of direct relevance to coronary artery disease and other human diseases. MDCs protect the pathogen, while the infection promotes further mDC differentiation and converts mDCs to an atherogenic phenotype. We have thus identified an important pathophysiological mechanism

that links chronic low grade infections to an increased risk of cardiovascular disease and other diseases.

Supplementary Material

Refer to Web version on PubMed Central for supplementary material.

Acknowledgments

Special thanks to Ruth Tenzler for study coordination and to Emil Kozarov for the post-mortem biopsies.

References

1. Naghavi M, Falk E, Hecht HS, Jamieson MJ, Kaul S, Berman D, Fayad Z, Budoff MJ, Rumberger J, Naqvi TZ, Shaw LJ, Faergeman O, Cohn J, Bahr R, Koenig W, Demirovic J, Arking D, Herrera VL, Badimon J, Goldstein JA, Rudy Y, Airaksinen J, Schwartz RS, Riley WA, Mendes RA, Douglas P, Shah PK. From vulnerable plaque to vulnerable patient--Part III: Executive summary of the Screening for Heart Attack Prevention and Education (SHAPE) Task Force report. *Am J Cardiol.* 2006; 98:2H–15H.
2. Vita JA, Loscalzo J. Shouldering the risk factor burden: infection, atherosclerosis, and the vascular endothelium. *Circulation.* 2002; 106:164–166. [PubMed: 12105150]
3. Pesonen E, El-Segaier M, Persson K, Puolakkainen M, Sarna S, Ohlin H, Pussinen PJ. Infections as a stimulus for coronary occlusion, obstruction, or acute coronary syndromes. *Thromb Haemostasis.* 2009; 3:447–454. [PubMed: 19773293]
4. Gibson FC 3rd, Yumoto H, Takahashi Y, Chou HH, Genco CA. Innate immune signaling and *Porphyromonas gingivalis*-accelerated atherosclerosis. *J Dent Res.* 2006; 85:106–121. [PubMed: 16434728]
5. Offenbacher S, Beck JD, Moss K, Mendoza L, Paquette DW, Barrow DA, Couper DJ, Stewart DD, Falkner KL, Graham SP, Grossi S, Gunsolley JC, Madden T, Maupome G, Trevisan M, Van Dyke TE, Genco RJ. Results from the Periodontitis and Vascular Events (PAVE) Study: a pilot multicentered, randomized, controlled trial to study effects of periodontal therapy in a secondary prevention model of cardiovascular disease. *J Periodontol.* 2009; 80:190–201. [PubMed: 19186958]
6. Beck JD, Offenbacher S. Systemic effects of periodontitis: epidemiology of periodontal disease and cardiovascular disease. *J Periodontol.* 2005; 76:2089–2100. [PubMed: 16277581]
7. Kshirsagar AV, Craig RG, Moss KL, Beck JD, Offenbacher S, Kotanko P, Klemmer PJ, Yoshino M, Levin NW, Yip JK, Almas K, Lupovici EM, Usvyat LA, Falk RJ. Periodontal disease adversely affects the survival of patients with end-stage renal disease. *Kidney Int.* 2009; 75:746–751. [PubMed: 19165177]
8. Zeituni AE, Carrion J, Cutler CW. *Porphyromonas gingivalis*-dendritic cell interactions: consequences for coronary artery disease. *Journal of Oral Microbiology.* 2010; 2:5782.
9. Zeituni AE, Jotwani R, Carrion J, Cutler CW. Targeting of DC-SIGN on human dendritic cells by minor fimbriated *Porphyromonas gingivalis* strains elicits a distinct effector T cell response. *J Immunol.* 2009; 183:5694–5704. [PubMed: 19828628]
10. Zeituni AE, McCaig W, Scisci E, Thanassi DG, Cutler CW. The native 67-kilodalton minor fimbria of *Porphyromonas gingivalis* is a novel glycoprotein with DC-SIGN-targeting motifs. *J Bacteriol.* 2010; 192:4103–4110. [PubMed: 20562309]
11. Perez-Chaparro PJ, Lafaurie GI, Gracieux P, Meuric V, Tamanai-Shacoori Z, Castellanos JE, Bonnefante-Mallet M. Distribution of *Porphyromonas gingivalis* fimA genotypes in isolates from subgingival plaque and blood sample during bacteremia. *Biomedica.* 2009; 29:298–306. [PubMed: 20128354]
12. Fine DH, Furgang D, McKiernan M, Tereski-Bischio D, Ricci-Nittel D, Zhang P, Araujo MW. An investigation of the effect of an essential oil mouthrinse on induced bacteraemia: a pilot study. *J Clin Periodontol.* 2010; 37:840–847. [PubMed: 20633071]
13. Li L, Michel R, Cohen J, Decarlo A, Kozarov E. Intracellular survival and vascular cell-to-cell transmission of *Porphyromonas gingivalis*. *BMC Microbiol.* 2008; 8:26. [PubMed: 18254977]

14. Randolph GJ. The fate of monocytes in atherosclerosis. *J Thromb Haemost.* 2009; 7(Suppl 1):28–30. [PubMed: 19630762]
15. Gautier EL, Jakubzick C, Randolph GJ. Regulation of the migration and survival of monocyte subsets by chemokine receptors and its relevance to atherosclerosis. *Arterioscler Thromb Vasc Biol.* 2009; 29:1412–1418. [PubMed: 19759373]
16. Bobryshev YV. Dendritic cells in atherosclerosis: current status of the problem and clinical relevance. *Eur Heart J.* 2005; 26:1700–1704. [PubMed: 15855191]
17. Weber C, Zernecke A, Libby P. The multifaceted contributions of leukocyte subsets to atherosclerosis: lessons from mouse models. *Nat Rev Immunol.* 2008; 8:802–815. [PubMed: 18825131]
18. Bobryshev YV, Lord RS. Ultrastructural recognition of cells with dendritic cell morphology in human aortic intima. Contacting interactions of Vascular Dendritic Cells in athero-resistant and athero-prone areas of the normal aorta. *Arch Histol Cytol.* 1995; 58:307–322. [PubMed: 8527238]
19. Cybulsky MI, Jongstra-Bilen J. Resident intimal dendritic cells and the initiation of atherosclerosis. *Curr Opin Lipidol.* 2010; 21:397–403. [PubMed: 20720490]
20. Paulson KE, Zhu SN, Chen M, Nurmohamed S, Jongstra-Bilen J, Cybulsky MI. Resident intimal dendritic cells accumulate lipid and contribute to the initiation of atherosclerosis. *Circ Res.* 2010; 106:383–390. [PubMed: 19893012]
21. Bobryshev YV. Dendritic cells and their role in atherogenesis. *Lab Invest.* 2010; 90:970–984. [PubMed: 20458277]
22. Bobryshev YV, Lord RS. Co-accumulation of dendritic cells and natural killer T cells within rupture-prone regions in human atherosclerotic plaques. *J Histochem Cytochem.* 2005; 53:781–785. [PubMed: 15928327]
23. Ziegler-Heitbrock L, Ancuta P, Crowe S, Dalod M, Grau V, Hart DN, Leenen PJ, Liu YJ, MacPherson G, Randolph GJ, Scherberich J, Schmitz J, Shortman K, Sozzani S, Strobl H, Zembala M, Austyn JM, Lutz MB. Nomenclature of monocytes and dendritic cells in blood. *Blood.* 2010; 116:e74–80. [PubMed: 20628149]
24. Merad M, Manz MG. Dendritic cell homeostasis. *Blood.* 2009; 113:3418–3427. [PubMed: 19176316]
25. Bonasio R, von Andrian UH. Generation, migration and function of circulating dendritic cells. *Curr Opin Immunol.* 2006; 18:503–511. [PubMed: 16777395]
26. Jotwani R, Cutler CW. Multiple dendritic cell (DC) subpopulations in human gingiva and association of mature DCs with CD4+ T-cells in situ. *J Dent Res.* 2003; 82:736–741. [PubMed: 12939360]
27. Jotwani R, Palucka AK, Al-Quotub M, Nouri-Shirazi M, Kim J, Bell D, Banchereau J, Cutler CW. Mature dendritic cells infiltrate the T cell-rich region of oral mucosa in chronic periodontitis: in situ, in vivo, and in vitro studies. *J Immunol.* 2001; 167:4693–4700. [PubMed: 11591800]
28. Yilmaz A, Lochno M, Traeg F, Cicha I, Reiss C, Stumpf C, Raaz D, Anger T, Amann K, Probst T, Ludwig J, Daniel WG, Garlachs CD. Emergence of dendritic cells in rupture-prone regions of vulnerable carotid plaques. *Atherosclerosis.* 2004; 176:101–110. [PubMed: 15306181]
29. Brown DL, Desai KK, Vakili BA, Nouneh C, Lee HM, Golub LM. Clinical and biochemical results of the metalloproteinase inhibition with subantimicrobial doses of doxycycline to prevent acute coronary syndromes (MIDAS) pilot trial. *Arterioscler Thromb Vasc Biol.* 2004; 24:733–738. [PubMed: 14962945]
30. Jongbloed SL, Kassianos AJ, McDonald KJ, Clark GJ, Ju X, Angel CE, Chen CJ, Dunbar PR, Wadley RB, Jeet V, Vulink AJ, Hart DN, Radford KJ. Human CD141+ (BDCA-3)+ dendritic cells (DCs) represent a unique myeloid DC subset that cross-presents necrotic cell antigens. *J Exp Med.* 2010; 207:1247–1260. [PubMed: 20479116]
31. Jotwani R, Cutler CW. Fimbriated *Porphyromonas gingivalis* is more efficient than fimbria-deficient *P. gingivalis* in entering human dendritic cells in vitro and induces an inflammatory Th1 effector response. *Infect Immun.* 2004; 72:1725–1732. [PubMed: 14977981]
32. Tonetti MS, D’Aiuto F, Nibali L, Donald A, Storry C, Parkar M, Suvan J, Hingorani AD, Vallance P, Deanfield J. Treatment of periodontitis and endothelial function. *N Engl J Med.* 2007; 356:911–920. [PubMed: 17329698]

33. Lafaurie GI, Mayorga-Fayad I, Torres MF, Castillo DM, Aya MR, Baron A, Hurtado PA. Periodontopathic microorganisms in peripheral blood after scaling and root planing. *J Clin Periodontol.* 2007; 34:873–879. [PubMed: 17850606]
34. Takeuchi Y, Aramaki M, Nagasawa T, Umeda M, Oda S, Ishikawa I. Immunoglobulin G subclass antibody profiles in Porphyromonas gingivalis-associated aggressive and chronic periodontitis patients. *Oral Microbiol Immunol.* 2006; 21:314–318. [PubMed: 16922931]
35. Tran SD, Rudney JD. Improved multiplex PCR using conserved and species-specific 16S rRNA gene primers for simultaneous detection of Actinobacillus actinomycetemcomitans, Bacteroides forsythus, and Porphyromonas gingivalis. *J Clin Microbiol.* 1999; 37:3504–3508. [PubMed: 10523542]
36. Savitt AG, Mena-Taboada P, Monsalve G, Benach JL. Francisella tularensis infection-derived monoclonal antibodies provide detection, protection, and therapy. *Clin Vaccine Immunol.* 2009; 16:414–422. [PubMed: 19176692]
37. Muthukuru M, Jotwani R, Cutler CW. Oral mucosal endotoxin tolerance induction in chronic periodontitis. *Infect Immun.* 2005; 73:687–694. [PubMed: 15664906]
38. Fan QST, Nakagawa T, Page RC. Antigenic cross-reactivity among Porphyromonas gingivalis serotypes. *Oral Microbiol Immunol.* 2000; 15:158–165. [PubMed: 11154398]
39. Kozarov E. Bacterial invasion of vascular cell types: vascular infectology and atherogenesis. *Future Cardiol.* 2012; 8:123–138. [PubMed: 22185451]
40. Migita K, Miyashita T, Maeda Y, Kimura H, Nakamura M, Yatsushashi H, Ishibashi H, Eguchi K. Reduced blood BDCA-2+ (lymphoid) and CD11c+ (myeloid) dendritic cells in systemic lupus erythematosus. *Clin Exp Immunol.* 2005; 142:84–91. [PubMed: 16178860]
41. Van Brussel I, Van Vre EA, De Meyer GR, Vrints CJ, Bosmans JM, Bult H. Decreased numbers of peripheral blood dendritic cells in patients with coronary artery disease are associated with diminished plasma Flt3 ligand levels and impaired plasmacytoid dendritic cell function. *Clin Sci (Lond).* 2011; 120:415–426. [PubMed: 21143200]
42. Epstein SE, Zhu J, Najafi AH, Burnett MS. Insights into the role of infection in atherogenesis and in plaque rupture. *Circulation.* 2009; 119:3133–3141. [PubMed: 19546396]
43. Alfakry H, Paju S, Sinisalo J, Nieminen MS, Valtonen V, Saikku P, Leinonen M, Pussinen PJ. Periodontopathogen- and host-derived immune response in acute coronary syndrome. *Scand J Immunol.* 2008; 74:383–389. [PubMed: 21645027]
44. Kozarov EV, Dorn BR, Shelburne CE, Dunn WA Jr, Progulské-Fox A. Human atherosclerotic plaque contains viable invasive Actinobacillus actinomycetemcomitans and Porphyromonas gingivalis. *Arterioscler Thromb Vasc Biol.* 2005; 25:e17–18. [PubMed: 15662025]
45. Svajger U, Obermajer N, Anderlüh M, Kos J, Jeras M. DC-SIGN ligation greatly affects dendritic cell differentiation from monocytes compromising their normal function. *J Leukoc Biol.* 2011; 89:893–905. [PubMed: 21447648]
46. Ramirez JA. Isolation of Chlamydia pneumoniae from the coronary artery of a patient with coronary atherosclerosis. The Chlamydia pneumoniae/Atherosclerosis Study Group. *Ann Intern Med.* 1996; 125:979–982. [PubMed: 8967709]
47. Johnson JL, Dwivedi A, Somerville M, George SJ, Newby AC. Matrix metalloproteinase (MMP)-3 activates MMP-9 mediated vascular smooth muscle cell migration and neointima formation in mice. *Arterioscler Thromb Vasc Biol.* 2011; 31:e35–44. [PubMed: 21719762]
48. Hollender P, Ittelett D, Villard F, Eymard JC, Jeannesson P, Bernard J. Active matrix metalloprotease-9 in and migration pattern of dendritic cells matured in clinical grade culture conditions. *Immunobiology.* 2002; 206:441–458. [PubMed: 12437074]
49. Distelmaier K, Adlbrecht C, Jakowitsch J, Winkler S, Dunkler D, Gerner C, Wagner O, Lang IM, Kubicek M. Local complement activation triggers neutrophil recruitment to the site of thrombus formation in acute myocardial infarction. *Thromb Haemost.* 2009; 102:564–572. [PubMed: 19718478]
50. Balogh S, Kiss I, Csaszar A. Toll-like receptors: link between “danger” ligands and plaque instability. *Curr Drug Targets.* 2009; 10:513–518. [PubMed: 19519353]
51. Niu J, Kolattukudy PE. Role of MCP-1 in cardiovascular disease: molecular mechanisms and clinical implications. *Clin Sci (Lond).* 2009; 117:95–109. [PubMed: 19566488]

52. Kume N. [New oxidized LDL receptors and their functions in atherogenesis]. *Nihon Ronen Igakkai Zasshi*. 2002; 39:264–267. [PubMed: 12073583]
53. Munk PS, Breland UM, Aukrust P, Skadberg O, Ueland T, Larsen AI. Inflammatory response to percutaneous coronary intervention in stable coronary artery disease. *J Thromb Thrombolysis*. 2011; 31:92–98. [PubMed: 20373128]
54. Jotwani R, Muthukuru M, Cutler CW. Increase in HIV receptors/co-receptors/alpha-defensins in inflamed human gingiva. *J Dent Res*. 2004; 83:371–377. [PubMed: 15111627]
55. Bobryshev YV, Lord RS. Expression of heat shock protein-70 by dendritic cells in the arterial intima and its potential significance in atherogenesis. *J Vasc Surg*. 2002; 35:368–375. [PubMed: 11854737]
56. Zhang Y, Ohashi N, Rikihisa Y. Cloning of the heat shock protein 70 (HSP70) gene of *Ehrlichia sennetsu* and differential expression of HSP70 and HSP60 mRNA after temperature upshift. *Infect Immun*. 1998; 66:3106–3112. [PubMed: 9632573]
57. Sims TJ, Lernmark A, Mancl LA, Schifferle RE, Page RC, Persson GR. Serum IgG to heat shock proteins and *Porphyromonas gingivalis* antigens in diabetic patients with periodontitis. *J Clin Periodontol*. 2002; 29:551–562. [PubMed: 12296783]
58. Soilleux EJ, Morris LS, Trowsdale J, Coleman N, Boyle JJ. Human atherosclerotic plaques express DC-SIGN, a novel protein found on dendritic cells and macrophages. *J Pathol*. 2002; 198:511–516. [PubMed: 12434421]
59. Gringhuis SI, den Dunnen J, Litjens M, van der Vlist M, Geijtenbeek TB. Carbohydrate-specific signaling through the DC-SIGN signalosome tailors immunity to *Mycobacterium tuberculosis*, HIV-1 and *Helicobacter pylori*. *Nat Immunol*. 2009; 10:1081–1088. [PubMed: 19718030]
60. Jotwani R, Eswaran SV, Moonga S, Cutler CW. MMP-9/TIMP-1 imbalance induced in human dendritic cells by *Porphyromonas gingivalis*. *FEMS Immunol Med Microbiol*. 2010; 58:314–321. [PubMed: 20030715]
61. Danzig V, Mikova B, Kuchynka P, Benakova H, Zima T, Kittnar O, Skrha J, Linhart A, Kalousova M. Levels of circulating biomarkers at rest and after exercise in coronary artery disease patients. *Physiol Res*. 2010; 59:385–392. [PubMed: 19681661]
62. Ng KT, Li JP, Ng KM, Tipoe GL, Leung WK, Fung ML. Expression of hypoxia-inducible factor-1alpha in human periodontal tissue. *J Periodontol*. 2011; 82:136–141. [PubMed: 21043802]
63. Weis M, Schlichting CL, Engleman EG, Cooke JP. Endothelial determinants of dendritic cell adhesion and migration: new implications for vascular diseases. *Arterioscler Thromb Vasc Biol*. 2002; 22:1817–1823. [PubMed: 12426210]
64. Cutler CW, Jotwani R. Dendritic cells at the oral mucosal interface. *J Dent Res*. 2006; 85:678–689. [PubMed: 16861283]
65. Olsen I. Update on bacteraemia related to dental procedures. *Transfus Apher Sci*. 2008; 39:173–178. [PubMed: 18753008]
66. Uehira K, Amakawa R, Ito T, Tajima K, Naitoh S, Ozaki Y, Shimizu T, Yamaguchi K, Uemura Y, Kitajima H, Yonezu S, Fukuhara S. Dendritic cells are decreased in blood and accumulated in granuloma in tuberculosis. *Clin Immunol*. 2002; 105:296–303. [PubMed: 12498811]
67. Urban BC, Cordery D, Shafi MJ, Bull PC, Newbold CI, Williams TN, Marsh K. The frequency of BDCA3-positive dendritic cells is increased in the peripheral circulation of Kenyan children with severe malaria 2006. 2006; 74:6700–6706.
68. Semnani RT, Mahapatra L, Dembele B, Konate S, Metenou S, Dolo H, Coulibaly ME, Soumaoro L, Coulibaly SY, Sanogo D, Seriba Doumbia S, Diallo AA, Traore SF, Klion A, Nutman TB, Mahanty S. Expanded numbers of circulating myeloid dendritic cells in patent human filarial infection reflect lower CCR1 expression. *J Immunol*. 2010; 185
69. Dua B, Watson RM, Gauvreau GM, O'Byrne PM. Myeloid and plasmacytoid dendritic cells in induced sputum after allergen inhalation in subjects with asthma. *J Allergy Clin Immunol*. 2010; 126:133–139. [PubMed: 20538329]
70. Shi H, Ge J, Fang W, Yao K, Sun A, Huang R, Jia Q, Wang K, Zou Y, Cao X. Peripheral-blood dendritic cells in men with coronary heart disease. *Am J Cardiol*. 2007; 100:593–597. [PubMed: 17697812]

71. Yilmaz A, Schaller T, Cicha I, Altendorf R, Stumpf C, Klinghammer L, Ludwig J, Daniel WG, Garlich CD. Predictive value of the decrease in circulating dendritic cell precursors in stable coronary artery disease. *Clin Sci (Lond)*. 2009; 116:353–363. [PubMed: 18808367]
72. Fukunaga T, Soejima H, Irie A, Fukushima R, Oe Y, Kawano H, Sumida H, Kaikita K, Sugiyama S, Nishimura Y, Ogawa H. High ratio of myeloid dendritic cells to plasmacytoid dendritic cells in blood of patients with acute coronary syndrome. *Circ J*. 2009; 73:1914–1919. [PubMed: 19644219]
73. Van Vre EA, Van Brussel I, de Beeck KO, Hoymans VY, Vrints CJ, Bult H, Bosmans JM. Changes in blood dendritic cell counts in relation to type of coronary artery disease and brachial endothelial cell function. *Coron Artery Dis*. 2010; 21:87–96. [PubMed: 20124992]
74. Rolland A, Guyon L, Gill M, Cai YH, Banchereau J, McClain K, Palucka AK. Increased blood myeloid dendritic cells and dendritic cell-poiectins in Langerhans cell histiocytosis. *J Immunol*. 2005; 174:3067–3071. [PubMed: 15728521]
75. Roth GA, Ankersmit HJ, Brown VB, Papapanou PN, Schmidt AM, Lalla E. Porphyromonas gingivalis infection and cell death in human aortic endothelial cells. *FEMS Microbiol Lett*. 2007; 272:106–113. [PubMed: 17459112]
76. Davies JM, Sheil B, Shanahan F. Bacterial signalling overrides cytokine signalling and modifies dendritic cell differentiation. *Immunology*. 2009; 128:e805–815. [PubMed: 19740342]
77. Rozen S, Skaletsky H. Primer3 on the WWW for general users and for biologist programmers. *Methods Mol Biol*. 2000; 132:365–386. [PubMed: 10547847]

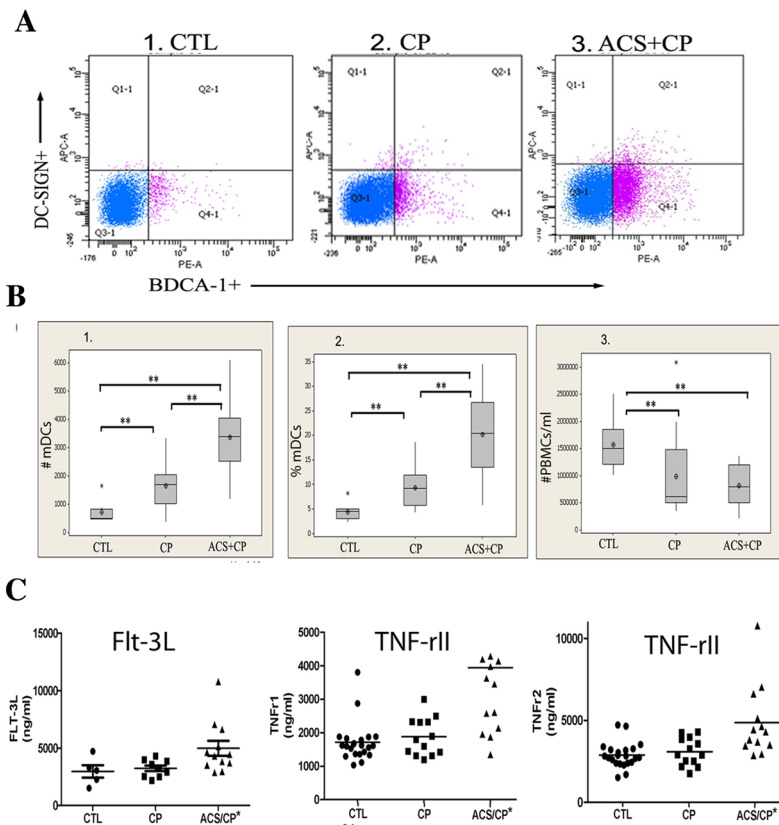
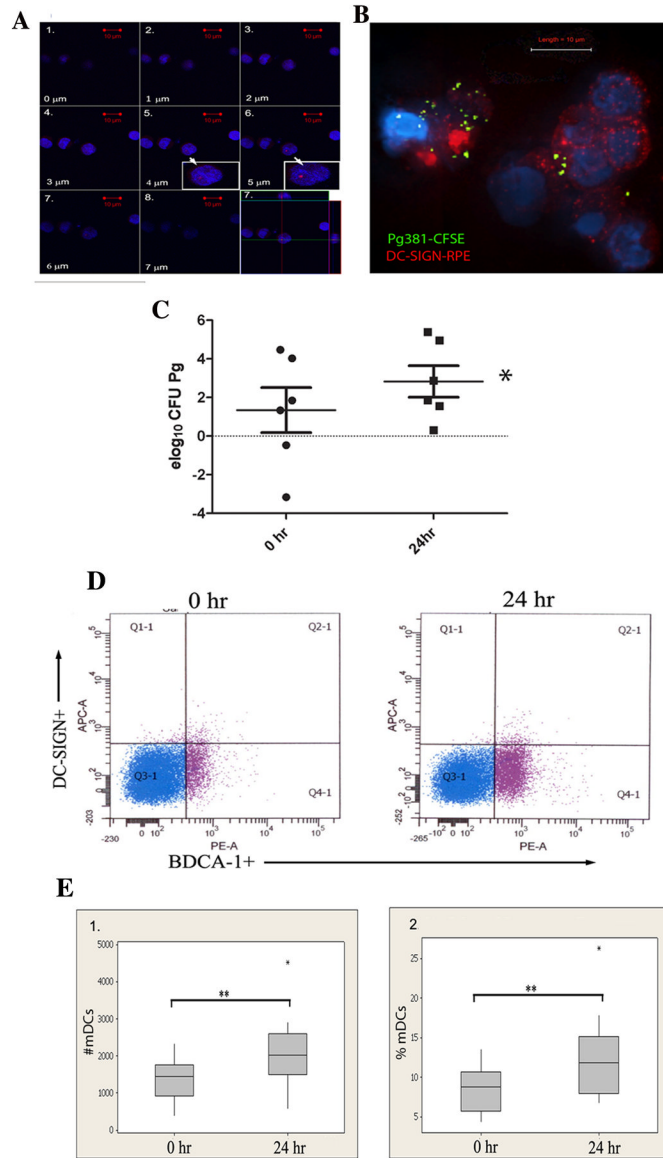
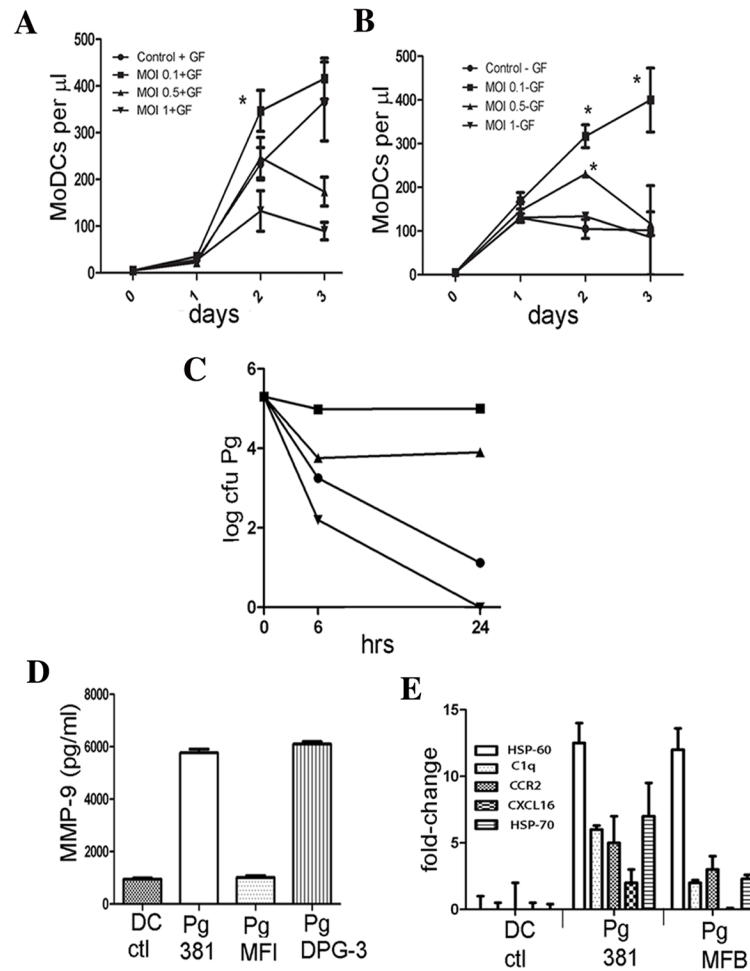


FIGURE 1. Increased blood mDC frequency in chronic periodontitis and acute coronary syndrome. **A.** Representative scattergrams from flow cytometry analysis of CD1c+ (BDCA-1) (x-axis) DC-SIGN+ (y-axis) blood mDCs at baseline in healthy control (CTL) subjects (n=25), chronic periodontitis (CP) subjects (n=25) and subjects with acute coronary syndrome and CP (ACS+CP) (n= 15). **B.** Mean numbers (panel 1) and percentages (panel 2) of blood mDCs (mDCs/20,000 PBMCs) and total numbers of PBMCs/ml (panel 3) in CP, ACS/CP relative to CTL. * p<0.05, Students t-test. **C.** Serum ELISA levels of FLT-3L, soluble TNFR-1, TNFR-2 (ng/ml) in all three patient groups performed in triplicate for each patient sample. *Significant difference in ACS+CP groups relative to CP and CTL (p<0.05, Students t-test).

**FIGURE 2.**

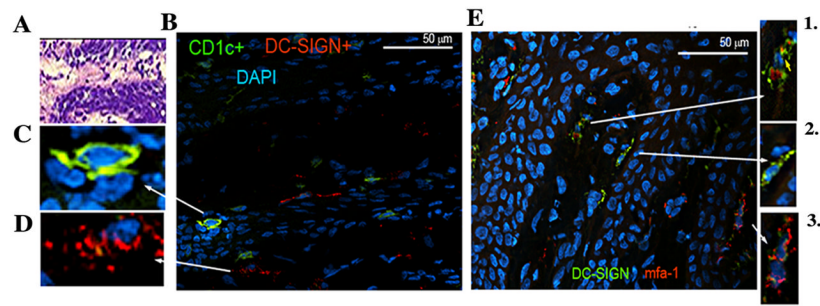
P. gingivalis carriage state and frequency of blood mDCs, before and after induced bacteremia. A. Image series from scanning laser confocal microscopy (panels 1–7, z-stack series of 1µm slices) of CD1c⁺ (BDCA-1⁺) blood mDCs from oral carriage positive CP patient, permeabilized and cytocentrifuged on slides and probed with AEZaMfa1-PE, followed by Vectashield™ mounting media. *P. gingivalis* (red) in mDC is shown by white arrow. B. Epifluorescence deconvolution image analysis of blood mDCs from a healthy donor pulsed in vitro with CFSE-labeled *P. gingivalis* 381 (green) at an MOI of 1 for 3 hours. MDCs were counterstained with DAPI (blue) and RPE-conjugated DC-SIGN (red). C. Significant increase in *P. gingivalis* 16s rDNA content of blood mDCs from CP subjects (n=6) 24 hours after local debridement (S&RP). MDCs were analyzed for 16s rDNA of *P. gingivalis*, quantified as in the supplementary methods. (*p=0.02, paired T-test). D. Representative scattergrams from flow cytometry analysis of CD1c⁺ (BDCA-1⁺), CD209 (DC-SIGN⁺) blood mDCs before (0hr) and 24 hours after local debridement (S&RP) of CP patients as described in materials and methods. E. Significant increase in mean number

(panel 1) and percentages (panel 2) of blood mDCs 24 hours after S&RP (per 30,000 PBMCs) (** $p < 0.05$, Paired t-test).

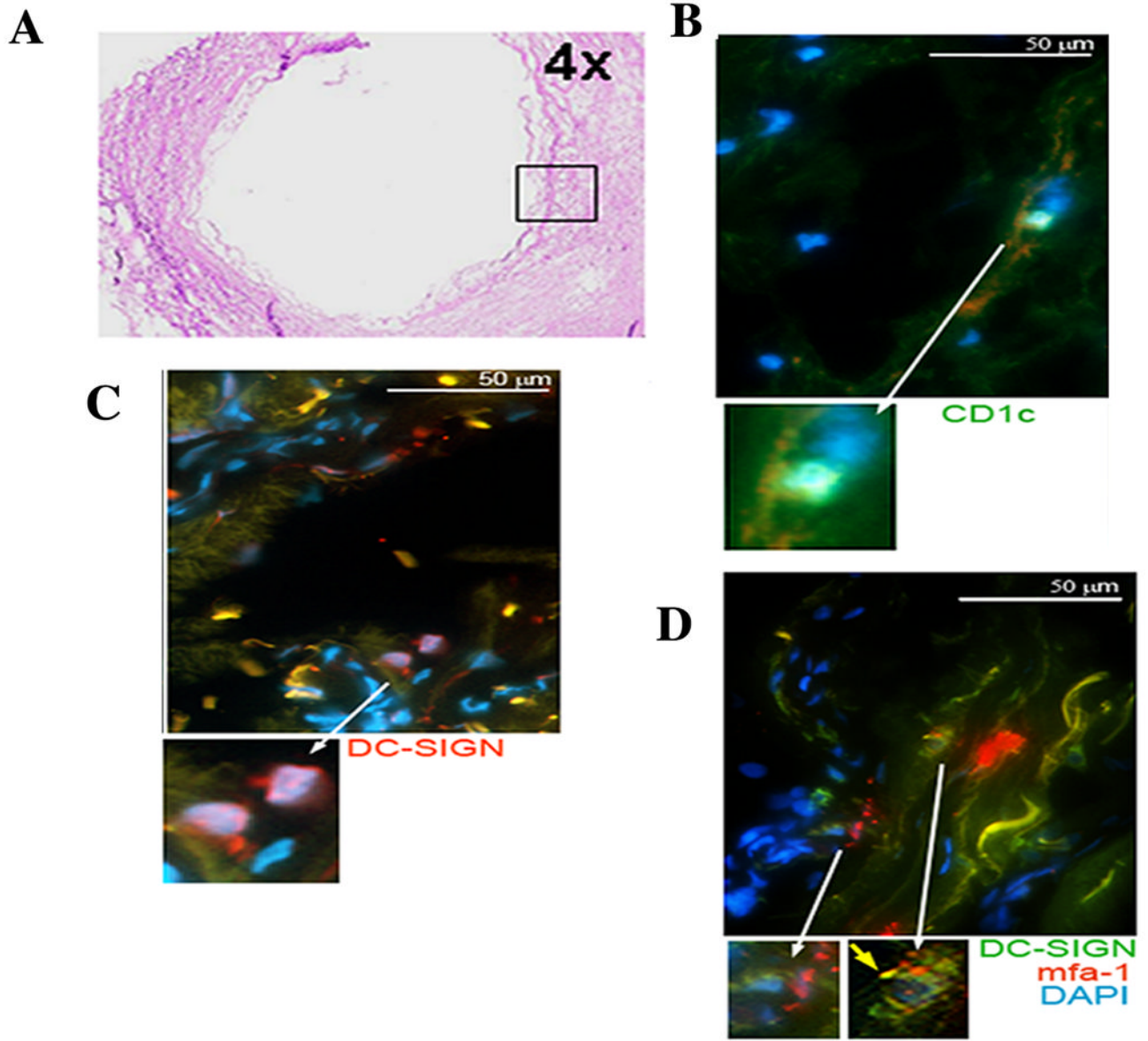
**FIGURE 3.**

P. gingivalis induces mDC differentiation, survives within mDCs and induces atherogenic mDC phenotype. A. Pre-DCs monocytes from healthy controls were cultured in triplicate with growth factors GM-CSF/IL-4 +/- *P. gingivalis* 381 at MOIs of 0.1, 0.5, and 1. The mean number of cells appearing in the MoDC gate (CD1c⁺DC-SIGN⁺) per $\mu\text{l} \pm$ S.E. is shown. Phenotype of immature MoDCs was further confirmed by evidence of downregulation of CD14 and low to no expression of CD83 and CCR7 (not shown). *Significant difference between control + GF (plus growth factors [GF]) and MOI of 0.1 + GF (ANOVA, $p < 0.05$). Data are representative of results of assay repeated three separate times. B. Performed as in A., but without growth factors. Significant differences were noted in mean # MoDCs per μl in MOI 0.1-GF vs. MOI 0.5 - GF at 2, 3 days, and in MOI 0.1 - GF, MOI 0.5 - GF vs control and MOI 1-GF at 2 days (ANOVA, $p < 0.05$). C. Wild type Pg381 was incubated in mDC buffer alone (filled circle) or with mDCs (filled square), or with mDCs pre-treated with cytochalasin D (filled triangle), or control PMNs (inverted filled triangle) at a multiplicity of infection of 100 for from 0, 6, 24 hours. Internalization of CFSE-labeled *P. gingivalis* was confirmed by epifluorescence microscopy. Cells were lysed and viable bacteria recovered on enriched anaerobic 5% blood agar plates in triplicate under anaerobic conditions (10% H₂, 5% CO₂ in nitrogen) at a 1:10 dilution at 35°C for 14 days after which Log₁₀ cfu/ml were determined. Experiment was repeated three separate times and data are representative of consistent results. D. MoDCs were pulsed with wild type Pg 381, its mfa-1 minor fimbriae deficient strain (MFI) or fimA major fimbriae deficient strain

(DPG-3) or no Pg (DC ctl) for 18 h at a MOI of 1:25. Secretion of MMP-9 in pg/ml were assessed by ELISA. The data are the mean \pm S.D. of triplicate assays. E. MoDCs were pulsed in triplicate with wild type Pg381, its fimbriae-less mutant MFB or no Pg (CTL) at a 25:1 MOI for 3 hrs and uptake of CFSE-labeled Pg monitored by FACS analysis (not shown). qRT-PCR (BioRad) was used to determine expression levels, normalized to β -actin and expressed as fold- changes in mRNA. PCR primers were designed using PRIMER3 Software (77). For relative quantification of transcript expression, Ct values were obtained for each gene and data were analyzed using the Excel (Microsoft) macro GENEX v1.10 (Gene Expression analysis for iCycle iQ®Real-time PCR Detection System, v1.10, 2004, Bio-Rad Laboratories).

**FIGURE 4.**

P. gingivalis infected mDCs in oral submucosa of CP patient A. Representative gingival tissue section (7 μ M thick) from a CP patient stained with hematoxylin and eosin (H&E) (20x). B. Section was stained with FITC-conjugated mouse anti-human CD1c (BDCA-1) and RPE-conjugated mouse anti-human CD209 (DC-SIGN) and image captured at 100x. C. Shown at ~500x final enlargement (optical and digital) is detail view of individual of CD1c+ mDC/LC in epithelium and D. DC-SIGN+ mDCs in lamina propria (200x). E. FITC-conjugated mouse anti-human CD209 and Alexa Fluor 594 conjugated to mfa-1 antibody AEZ α Mfa1 using commercial DyLightTM microscale antibody labeling kit in CP oral mucosal tissues (100x). Shown in panels 1–3 (at 200x) are detail of areas of mfa-1-DC-SIGN colocalization.

**FIGURE 5.**

P. gingivalis infected mDCs in atherosclerotic plaque of CP patient A. Representative post-mortem coronary artery 7 μM tissue section from ACS/CP patient stained with H&E, image obtained with enhanced light microscopy (Nikon E600) (4x). B. CAD tissue sections were stained with FITC-conjugated CD1c+, C. RPE-conjugated DC-SIGN+ and D. DC-SIGN-mfa-1 dual staining using FITC-conjugated DC-SIGN+ and Alexa Fluor 594 conjugated-mfa-1. Prior to staining, all tissue sections were blocked with 5% BSA in PBS, along with anti-human FcR block reagent. Appropriate controls included isotype matched antibodies and pre-immune antibodies (not shown). All sections were mounted with VectaShield mounting medium containing DAPI. Images were acquired with a Zeiss LSM 510 META NLO Two-Photon Laser Scanning Confocal Microscope System.

Table

Clinical Description, Demographics, Serum Lipids, Cytokines

Clinical Description	Patient Cohorts		
	Control (n=25)	CP (n=25)	ACS/CP (n=15)
	<ul style="list-style-type: none"> • non-smokers • without CP • no ACS, diabetes, cancer or other reported systemic disease 	<ul style="list-style-type: none"> • moderate to severe CP • >20 teeth, • 8 with probing depth > 4mm • ALOSS > 3mm, BOP, alveolar bone crest > 3 mm from CEJ, Non-diabetic, non-smoker 	<ul style="list-style-type: none"> • troponin+ unstable angina • ECG evidence of ischemia • 1, 2 or 3-vessel CAD, history of MI • moderate to severe CP • <u>Excluded</u> previous coronary bypass, untreated or incomplete treatment of coronary artery disease, life expectancy of <2 years.
Age years			
Median (range)	51 (38–63)	52 (31–72)	65 (32–89)
Gender			
Males	12	11	10
Females	13	14	5
Self-reported race or ethnic group (%)			
White	12 (48)	16 (64)	11 (63)
Black	9 (36)	2 (8)	0 (0)
Asian	0 (0)	2 (8)	0 (0)
Hispanic	4 (16)	4 (16)	4 (27)
Arab	0 (0)	1 (4)	0 (0)
Serum Lipids (mg/dl)			
Triglycerides	102 ± 8.3	155 ± 16 *	146 ± 17
Total Cholesterol	209 ± 8	215 ± 9	170 ± 11
LDL	119 ± 7	134 ± 8	96 ± 9.1
HDL	70 ± 4	50 ± 3 *	42 ± 11
CHOL/HDL ratio	3.2 ± 0.2	4.6 ± 0.3 *	4.2 ± 0.9
VLDL	20.3 ± 1.6	31 ± 3 *	27 ± 4
Serum Cytokines			
FLT-3L (pg/ml)	65 ± 24	66 ± 18	137 ± 27 †

Patient Cohorts			
TNFr-I (pg/ml)	1750 ± 564	1850 ± 867	3520 ± 2100
TNFr-II (pg/ml)	2969 ± 537	3239 ± 247	4982 ± 647 †
hsCRP (ng/ml)	2293 ± 1046	2797 ± 525	2851 ± 413
Serum IgG titer against <i>P. gingivalis</i> DPG-3			
Anti-Pg IgG	1.06 ± 0.06	2.69 ± 0.19 *	n.d.

n.d. not determined;

* Significantly elevated vs. CTL (p<0.05, Students t-test)

† Significantly elevated vs. CP and CTL (p<0.05, Students t-test)